JOURNAL OF APPLIED ELECTROCHEMISTRY 14 (1984) 449–458

Solid state electro-oxidation processes on lead and lead alloys in the $PbO_2/PbSO_4$ regions

E. HAMEENOJA*, N. A. HAMPSON

Department of Chemistry, University of Technology, Loughborough, Leicestershire, LE11 3TU, UK

Received 25 September 1983

The results are presented of potential step experiments in 5M sulphuric acid on lead and two lead alloys of some commercial importance. Differences in the nucleation and growth processes of PbO_2 on $PbSO_4$ are observed as a result of the presence of the alloying ingredient. The effect of Sb is very marked. Some reasons for the observations are discussed.

Nomenclature

A time dependent rate of nucleation
F Faraday constant
i_m maximum current
k_1 parallel rate constant
k_2 orthogonal rate constant
M molecular weight
N_0 initial number of nuclei
t_m time corresponding to maximum current
z number of electrons transferred
ρ density

1. Introduction

For maintenance-free batteries, low self-discharge rate and minimal gassing are indispensable qualities. By replacing antimonial grid material with lead–calcium alloys the hydrogen overvoltage of the negative electrode is increased, however, new problems arise because the beneficial effect of antimony on the cycle life of the cell is lost. The purpose of this work is to study the influence of the grid alloy on the lead dioxide formation in order to see if there are any differences between the nucleation and growth mechanisms and whether these differences explain any of the effects observed in practice.

The mechanism of the formation of lead dioxide on the lead sulphate layer was first studied by Fleischmann and Thirsk [1]. Lead sulphate was potentiostatically formed on lead electrodeposited onto copper-plated platinum. The oxidation of the lead sulphate appeared to be controlled by a nucleation and three-dimensional crystal growth with an overlapping effect. Casson *et al.* [2, 3] used an electrodeposited β-PbO_2 electrode in order to follow the situation in general battery operation where the lead sulphate rests on a lead dioxide base. After the first reduction to the lead sulphate region there was no evidence found for nucleation processes because the underlying lead dioxide provided adequate centres for the growth of the lead dioxide [2].

In the experiments where the electrodes was maintained in the lead sulphate region for one hour [3] the oxidation mechanism was a three-dimensional growth with progressive nucleation in agreement with the results of Fleischmann and Thirsk [1]. The reoxidation of the electrode changed the mechanism into two successive instantaneous reactions. Hampson *et al.* [4] found that with the cycled lead electrode the oxidation transient indicates that the PbO_2 formation is a two-dimensional instantaneous nucleation process with subsequent overlap of growing centres. In the case of antimonial lead two current peaks in the transient revealed two two-dimensional instantaneous nucleation and growth processes.

It was decided to investigate the behaviour of a lead dioxide electrode on a lead alloy base which might result from continuous charge/discharge battery operation. Consequently, in this work, the flat electrodes (Pb, Pb–Sb, Pb–Ca–Sn) which had

*On study leave from Department of Chemistry, Helsinki University of Technology, Finland.

0021–891X/84 $03.00 + .12

been potentiodynamically cycled between the lead sulphate and lead dioxide region to a stabilized response were employed.

2. Experimental details

Experiments were performed with pure lead, lead–antimony (1.88 wt%) and lead–calcium (0.086 wt%) – tin (0.34 wt%) electrodes (A = 0.071 cm^2) mounted in Teflon. The electrodes were first mechanically polished on roughened glass and filter paper followed by a short (5 s) chemical etch in nitric acid (10%) and a thorough washing in tri-distilled water.

The counter-electrode was a pure lead (99.99%) rod with a large surface area compared with the working electrodes. Potentials were measured with reference to a Hg/Hg_2SO_4 electrode in sulphuric acid of the same concentration as the working solution (5M H_2SO_4).

Cycling of the electrodes and the potential step studies were made with a potentiostat (HI-TEK DT2 101) in conjunction with a function generator (Kemitron P61). The electrodes could be rotated at a uniform speed using a rotating disc assembly (Kemitron Electronics RD1). The voltammograms and the transient curves were recorded graphically (Houston 2000, XYt recorder). The data was analysed by means of a microcomputer (Kemitron 3000, Z-80, microprocessor based 64K system).

Prior to the potential step experiments, the working electrodes were cycled (50 mV s^{-1}) between 600 and 1250 mV for 4 h. After this time, stabilized voltammograms were obtained. It should be noted in this connection that in the first cycle it was necessary to raise the potential to 2000 mV in order to initiate PbO_2 formation. After cycling, the electrode was maintained in the lead sulphate region (500 and 600 mV) for ten minutes before an oxidative step to the lead dioxide region (1250 mV) was made. It was found that after following the current–time transient for 140 s a low constant current, probably due to oxygen evolution, was reached. After that time, the potential was stepped back to the lead sulphate region and the experiment was repeated. Experiments were made both with 500 and 600 mV as the initiated potential. In order to determine if there are any solution reactions limiting the rate of the oxidation, the whole series of experiments was repeated rotating the electrode (2 rps).

3. Results and discussion

3.1. *Potentiodynamic curves*

Fig. 1 shows the stabilized voltammograms of the Pb, Pb–Sb and Pb–Ca–Sn electrodes. The broadening of the peaks indicates the porous nature of the lead dioxide deposit which results from continued cycling between the $PbSO_4$ and the PbO_2 states. The shape of the lead–antimony voltammogram (B) reveals the most developed porosity. The peak potential (E_p) of the $PbSO_4$/PbO_2 oxidation reaction has decreased in the case of alloys as observed earlier [5]. The average E_p-values (at least eight measurements with each alloy) are 1095 ± 10 mV for pure lead, 1066 ± 10 mV for lead–antimony and 1078 ± 10 mV for lead–calcium–tin. The deviation in the values shows that the reaction is sensitive to irregularities in the surface structure. The highest peak currents were always obtained from Pb–Ca–Sn alloy and the lowest from Pb–Sb.

Table 1 shows the charge contained in the voltammograms of Fig. 1.

The charge contents of the positive and negative going sweeps are similar, any differences between the values being due to the inaccuracy of the

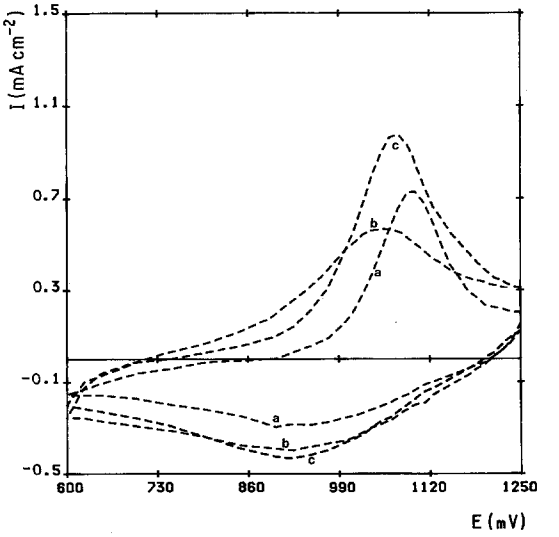

Fig. 1. Stabilized voltammograms for pure lead (a), lead–antimony (b) and lead–calcium–tin (c) after 4 h cycling between 600 and 1250 mV.

Table 1. The charge content of the positive and negative going sweeps of the stabilized voltammograms (Fig. 1). Sweep rate: 50 mV s^{-1}

Alloy	*Charge (mC cm^{-2})*	
	Positive going	*Negative going*
Pb	2.4	2.5
Pb–Sb	3.4	3.5
Pb–Ca–Sn	3.9	3.7

graphical determination of the area. The greater charge content for the alloys shows reaction in a thicker (more extensive) lead dioxide/lead sulphate film compared with that developed on the pure lead.

3.2. *Potentiostatic step experiments*

3.2.1 Pure lead. Fig. 2 shows the current–time transient curves of one series of experiments with the pure lead electrode. The behaviour is typical of all the results.

There was no evidence of any rotation speed dependence which means that the $PbSO_4$ oxidation reaction is only limited by a solid state nucleation and growth mechanism. This is also valid for alloys.

The peak current is the greatest in the first potentiostatic step from 600 mV (1a of Fig. 2). In the second step (1b of Fig. 2) the position of the current maximum is displaced to a longer time and the current output has diminished. The charge contained in the peak has increased however (Table 2). This means that during the 140 s 'stand' in the lead dioxide region (1250 mV) in the first step the thickness of the 'reacting' lead dioxide layer has been increased. Consequently for the second step the lead/lead sulphate boundary when the oxidation reaction starts must be 'deeper' in the electrode. Hence the maximum current is reached later but the total charge in the reaction is more than in the first step.

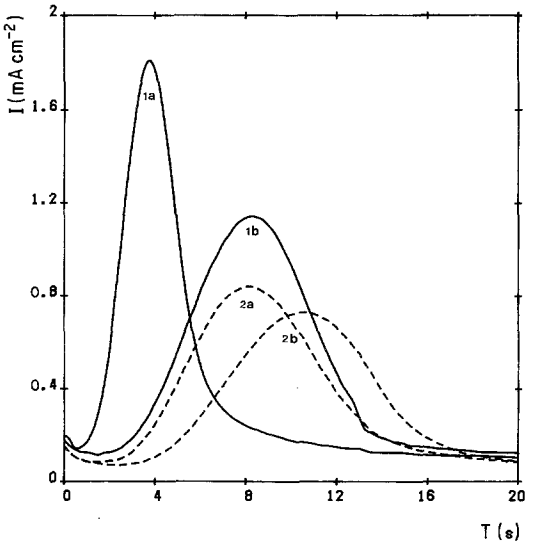

Fig. 2. Current–time curves of the pure lead electrode corresponding to the first (1a) and second (1b) steps from 600 to 1250 mV and the first (2a) and second (2b) steps from 500 to 1250 mV.

The shift to 500 mV as the initial potential of the step (2a of Fig. 2) decreases the current maximum and increases the charge content of the peak compared with the first step of 600 mV. The explanation is that going to a more negative potential in the lead sulphate region either changes the structure of the formed lead sulphate layer or increases its thickness. In this case, holding in the lead dioxide region (1250 mV) does not have the same influence as in the steps from 600 mV, the

Table 2. The position of the maximum current (t_m), the maximum current (i_m) and the charge contained in the main oxidation peak of lead sulphate to lead dioxide for the case of a pure lead electrode (mean values)

Oxidation step	t_m *(s)*	i_m *(mA cm^{-2})*	*Charge (mC cm^{-2})*
1. 600–1250 mV	3.8 ± 0.4	1.7 ± 0.2	5.8 ± 0.2
*2. 600–1250 mV	7.2 ± 1.0	1.2 ± 0.2	8.2 ± 0.2
1. 500–1250 mV	7.4 ± 1.0	0.6 ± 0.1	6.8 ± 0.4
*2. 500–1240 mV	10.4 ± 2	0.6 ± 0.2	6.8 ± 0.7

*2 is not a replicate of the first step but points to the following oxidation step in the same potential.

charge obtained in the second step from 500 mV being about the same as in the first step.

Comparing the charge values of the oxidation peaks shown in Table 2 with a charge of 325 $\mu C\ cm^{-2}$ [6] required to form a monolayer of $PbSO_4$ we can conclude that the formation of a multilayer of the thickness of approximately twenty layers of PbO_2 occurs.

The shape of the transients (Fig. 2) indicates a progressive nucleation and growth mechanism with subsequent overlapping of the growing centres [7]. In order to determine the dimensionality of the growth the current–time relationship in the rising part of the transient was analysed. In the case of three-dimensional progressive nucleation and growth i–t^3-dependence is observed [1, 3], while two-dimensional progressive mechanism shows i–t^2-behaviour [7]. We have found it convenient to deal in detail with the analysis of the first steps (from 600 to 500 mV) since the second steps simply show the same nucleation and growth mechanisms with a longer delay before the rise of the main transient.

Figs. 3 and 4 show that the first points of the rising transients give an equally satisfactory linear fit with both i–t^2- and i–t^3-dependence. We interpret this as a three-dimensional process with some growth restrictions in one dimension (see below).

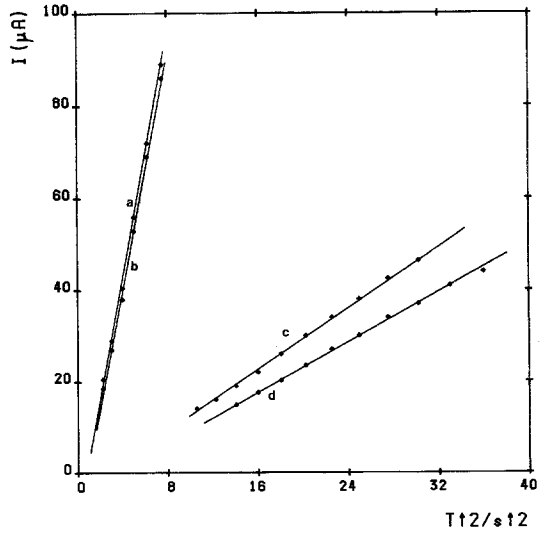

Fig. 3. Current vs t^2 for the rising part of the transient for the potentiostatic steps from 600 (a, b) and 500 (c, d) to 1250 mV with the cycled pure lead electrode.

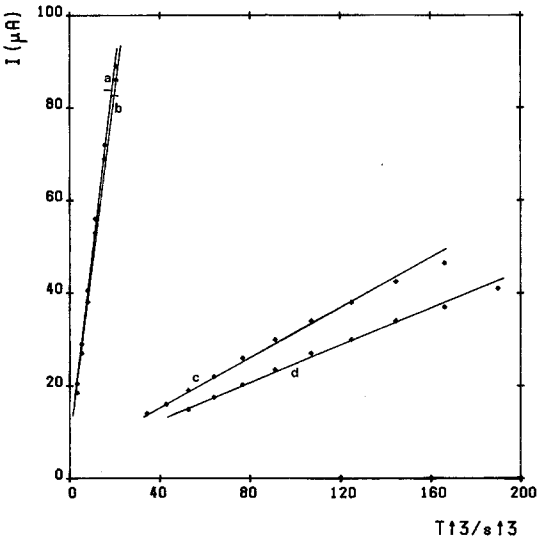

Fig. 4. As for Fig. 3 but showing current vs t^3.

The mechanisms were further studied by comparing the experimental data with the theoretical equations for two-dimensional progressive nucleation and growth [7]:

$$i = (zF\pi M/\rho)hAk^2t^2 \times \exp(-\pi M^2Ak^2t^3/3\rho^2) \qquad (1)$$

and three-dimensional growth of circular cones

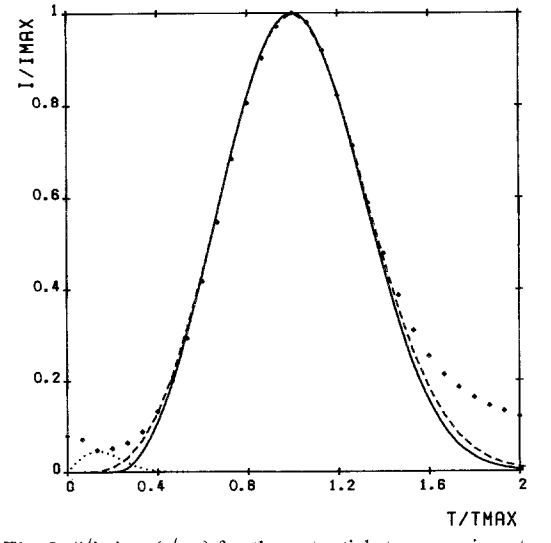

Fig. 5. (i/i_m) vs (t/t_m) for the potential step experiment from 600 to 1250 mV with the cycled pure lead electrode: the experimental points (●●●), 2D-progressive (——), 3D-progressive (-----), the initial 2D instantaneous (.....).

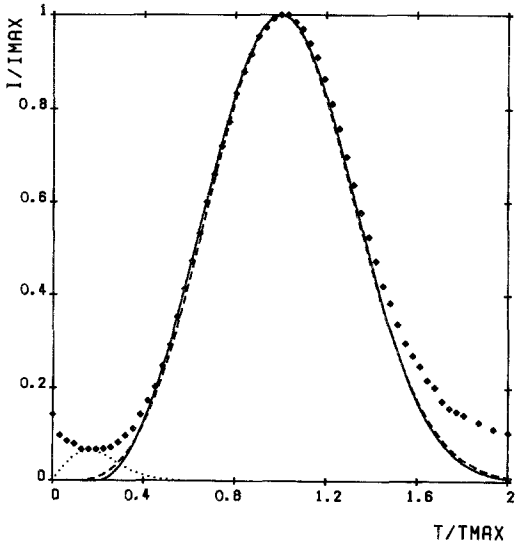

Fig. 6. As for Fig. 5 but for the potential step from 500 to 1250 mV.

with progressive nucleation first studied by Armstrong *et al.* [8]:

$$i = zFk_2[1 - \exp(-\pi M^2 k_1^2 A t^3/3\rho^2)] \times \exp(-\pi M^2 k_1^2 A t^3/3\rho^2) \quad (2)$$

Equations 1, 2 and the experimental results are shown in Figs. 5 and 6 in the form of the dimensionless plot of i/i_m vs t/t_m. The values are corrected for the residual current found after 140 s in the lead dioxide region (1250 mV) probably due to the oxygen evolution reaction. By setting $di/dt = 0$ the equations for i_m and t_m result. These have been replaced in the original equations so that the only parameters necessary for fitting are i_m and t_m.

As concluded for the initial rise of the transient both the two- and three-dimensional progressive nucleation and growth give a good fit with the 'main' oxidation peak (see Figs. 5, 6). In the two dimensional case it was necessary to introduce an induction time (600 mV: 0.8 s; 500 mV: 1.5 s) before the rise of the transient. A clearly discernable preference for either of the mechanisms is not apparent. From the evidence (charge) of the formation of a multilayer we nevertheless conclude that the three-dimensional model describes the process better than the two-dimensional one. If the growth perpendicular to the electrode surface is restricted by comparison with the growth parallel to the surface the observed result would apply.

The nucleation and growth mechanism does not change with the shift from 600 to 500 mV as the 'starting' potential for the step (see Fig. 6).

Evidently the 'main' oxidation processes discussed are inadequate for the complete description of the behaviour of the electrode near zero time or in the region exceeding $2 \times t_m$.

The current 'spike' observed at the beginning of the transient is comparatively high and the size of it is dependent on the alloy material (see below). This indicates that it contains not only the double layer charging current but also some elements of the chemical reaction current. With this in mind, it was found possible to separate out from the complex transient a small nucleation and growth process at the beginning of the main current controlling electrodeposition (Figs. 5, 6).

The deconvolution of the transient was made with the aid of the first part of the theoretical curve corresponding to the three-dimensional nucleation and growth process. Subtracting this curve from the experimental points reveals that the main process is likely to be preceded by a two-dimensional instantaneous nucleation and growth reaction [7]:

$$i = (zF\pi M/\rho)N_0 k^2 t \times \exp(-\pi M^2 N_0 k^2 t^2/\rho^3) \quad (3)$$

The charge content of the assumed instantaneous process is only about 1/30th part of the charge in the main process which means that less than one whole monolayer of PbO_2 is formed. The interpretation could be that before the oxidation progressively advances to the $PbSO_4$-layer a fast instantaneous nucleation of PbO_2 occurs in the boundary between the lead base and lead sulphate at specific growth points. The difference between the theoretical curves and the experimental data at times exceeding t_m (Figs. 2, 5, 6) is probably due to the slow growth (perhaps the recrystallization of the PbO_2-film) of the PbO_2 by a high-field conduction process.

3.2.2. Lead–antimony alloy. The current–time transients for the lead–antimony electrode are shown in Fig. 7. The initial rise of the current in all the experiments is very abrupt compared with pure lead and the lead–calcium–tin electrodes. The shape of the transient in the first potentiostatic step from 600 to 1250 mV (1a of Fig. 7)

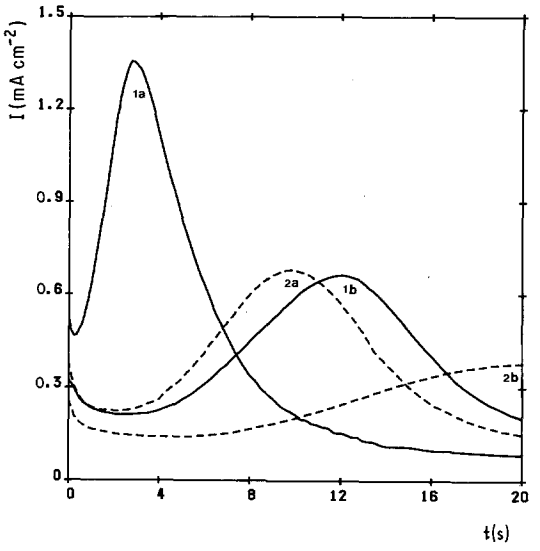

Fig. 7. Current–time curves of the lead–antimony electrode corresponding to the first (1a) and second (1b) steps from 600 to 1250 mV and the first (2a) and second (2b) steps from 500 to 1250 mV.

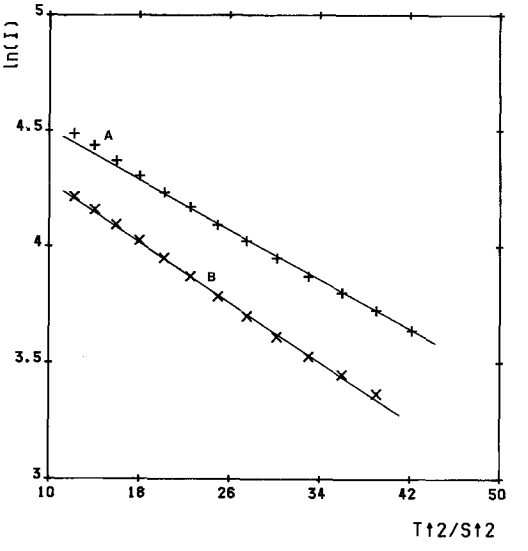

Fig. 8. ln i vs t^2 for the falling part of the transient for the potentiostatic step from 600 to 1250 mV with the lead–antimony electrode. (The replicate experiments A, B).

indicates an instantaneous nucleation and growth mechanism while the other transients appear to have progressive nucleation characteristics.

Table 3 shows that the position of the maximum current is changed remarkably in the second oxidation steps after a 140 s stand in the lead dioxide region (1250 mV). The value of the maximum current is only about half the value in the first step.

The amount of charge in the main oxidation reaction increases both in the second step from 600 mV and with the shift to 500 mV as the 'starting' potential. This indicates that the $PbSO_4$/PbO_2-layer on the electrode has thickened in both cases. In the first oxidation steps from 600 and 500 mV the charge content exceeds the values obtained for the pure lead electrode (see Tables 2, 3) in agreement with the analyses of the potentiodynamic curves showing greater reactivity for the alloys.

Because of the pronounced overlapping of the initial reactions we were not able to analyse the i–t behaviour for the rising part of the main peak in the potentiostatic step from 600 mV (1a of Fig. 7). In Figs. 8 and 9 the falling parts of the transients are represented by plotting ln i vs t^2 and ln (i/t) vs t^2 corresponding to two- and three-dimensional instantaneous nucleation and growth processes. Satisfactory straight lines confirm that with the lead–antimony electrodes the nucleation process is instantaneous in the step from 600 to 1250 mV. The crystal growth is of intermediate two- and three-dimensional character. The explanation is the same as in the case of pure lead.

Figs. 10 and 11 represent two of the four replicate experiments with lead–antimony from

Table 3. The position of the maximum current (t_m), *the maximum current* (i_m) *and the charge contained in the main oxidation peak of lead sulphate to lead dioxide on the lead–antimony electrode*

Oxidation step	t_m (*s*)	i_m (*mA cm*$^{-2}$)	*Charge* (*mC cm*$^{-2}$)
1. 600–1250 mV	2.7 ± 0.4	1.3 ± 0.2	6.7 ± 0.2
2. 600–1250 mV	12.0 ± 0.5	0.6 ± 0.1	7.9 ± 0.7
1. 500–1250 mV	10.5 ± 0.7	0.8 ± 0.1	7.6 ± 0.5
2. 500–1250 mV	21.8 ± 3	0.4 ± 0.1	6.2 ± 1.0

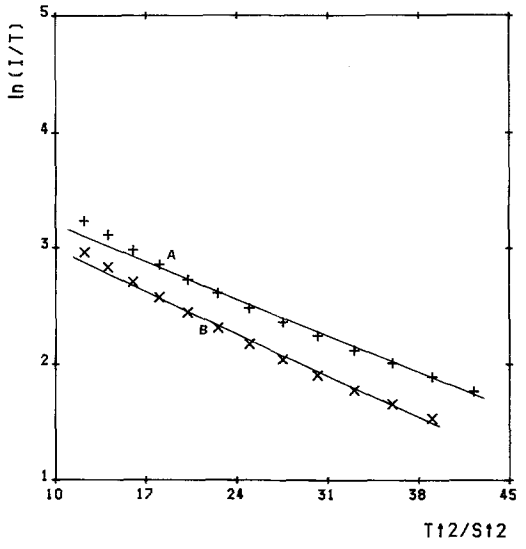

Fig. 9. As for Fig. 8 but for ln (i/t) vs t^2.

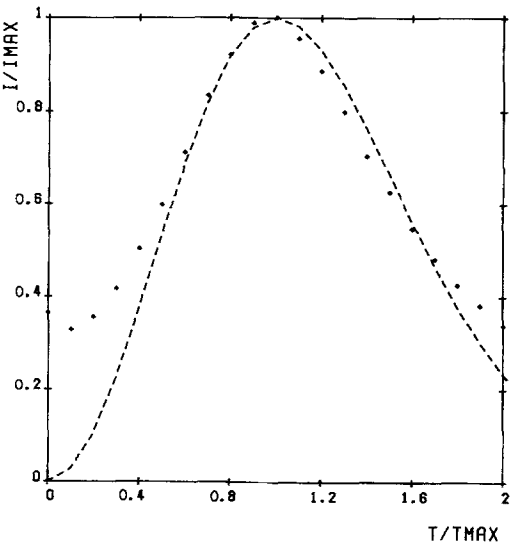

Fig. 11. As for Fig. 10: experimental points (●●●), 3D instantaneous (----).

600 mV. The one having the smallest charge content gives a good fit with the two-dimensional instantaneous nucleation and growth (see Fig. 10) and the other with greater charge content (see Fig. 11) with the three-dimensional instantaneous mechanism [8]:

$$i = zFk_2[1 - \exp(-\pi N_0 k_1^2 M^2 t^2/\rho^2)] \times \exp(-\pi N_0 k_1^2 M^2 t^2/\rho^2) \quad (4)$$

Repeating the potential step from 600 mV changes the nucleation mechanism (see Fig. 7). The stand (140 s) in the lead dioxide region (1250 mV) does not only thicken the PbO_2-film but some recrystallization process has to occur. In the second step from 600 mV the fast instantaneous nucleation is replaced by a progressive nucleation in the main oxidation peak. The size of the initial spike also

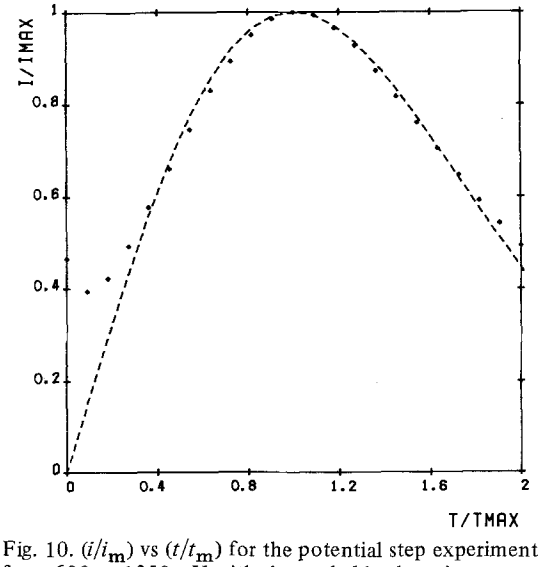

Fig. 10. (i/i_m) vs (t/t_m) for the potential step experiment from 600 to 1250 mV with the cycled lead–antimony electrode: the experimental points (●●●), 2D instantaneous (-----).

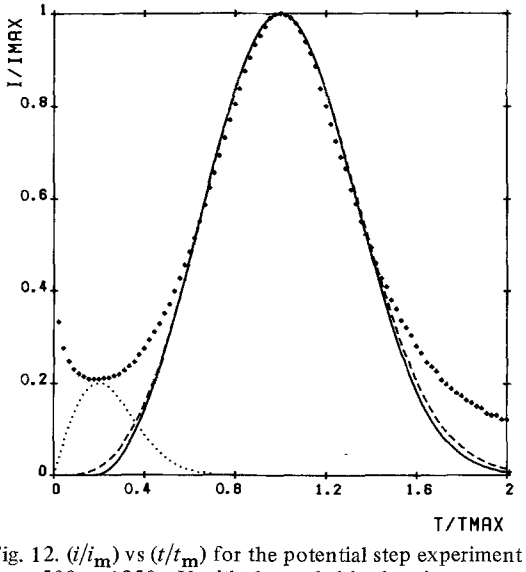

Fig. 12. (i/i_m) vs (t/t_m) for the potential step experiment from 500 to 1250 mV with the cycled lead antimony electrode: the experimental points (●●●), 2D progressive (——), 3D progressive (-----), the initial 2D instantaneous (.....).

decreases (1a, b of Fig. 7). A similar change occurs when the potentiostatic step is made from 500 to 1250 mV. It can be concluded that the number of nucleation centres for PbO_2 has diminished with the shift to a more negative potential.

Fig. 12 shows the experimental data for the step (500 → 1250 mV) together with the theoretical curves for two- and three-dimensional progressive nucleation and growth. Again, the fit for the three-dimensional process is only slightly better than for the two-dimensional one with the induction time of 2 s before the rise of the transient. The participation of the initial reactions is significant. Using the same deconvolution procedure as before the two-dimensional instantaneous nucleation and growth reaction at the beginning of the transient was separated out of the experimental *i–t*-curve (see Fig. 12). The charge contained in this peak is about one 10th of the charge in the main peak indicating an initial formation of two monolayers of PbO_2, approximately. Before the reaction advances to the $PbSO_4$-layer with a smaller number of nucleation centres compared with the step from 600 mV the oxidation process only occurs in the region next to the lead base. The total reaction is much slower than the instantaneous process in the potentiostatic step from 600 mV (see Table 3). In spite of the limited deconvolution the very first part of the transient still remains without an interpretation. However, because of the changes of its size with different alloys and overpotentials, we conclude that it is mostly due to a solid state activation process of the lead sulphate film.

Repeating the oxidation step from 500 mV results in a very slow reaction with a low current output (see Fig. 7 and Table 3).

3.2.3. Lead–calcium–tin. The typical current–time curves of the lead–calcium–tin electrodes

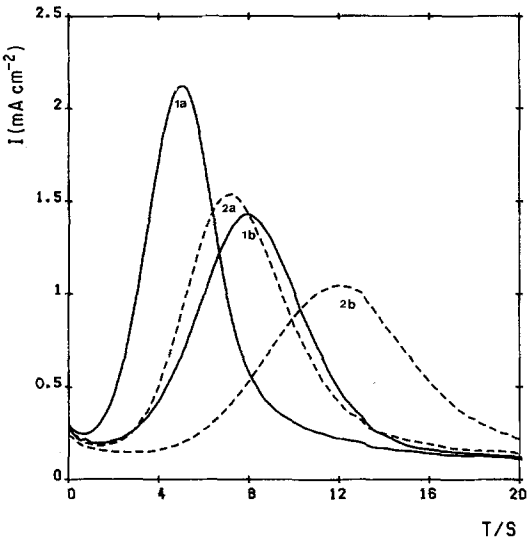

Fig. 13. Current–time curves of the lead–calcium–tin electrode corresponding to the first (1a) and second (1b) steps from 600 to 1250 mV and the first (2a) and second (2b) steps from 500 to 1250 mV.

are represented in Fig. 13. The behaviour of the alloy rather resembles pure lead than the lead–antimony alloy. The nucleation process is progressive in all the experiments. The position of the current peak in the successive pulses from the same potential is not changed as significantly as in the case of lead–antimony electrodes which means that lead–calcium–tin is less sensitive for the stand in the lead dioxide region (1250 mV) than antimonial alloy.

The values of the maximum currents and the charge contents of the main oxidation peaks are greater than those of the pure lead electrodes showing an increased thickness of the developed (passivating) layer (Table 4).

The deviation of the current and charge values between the replicate experiments is greater with Pb–Ca–Sn than with pure lead or Pb–Sb (see

Table 4. The position of the maximum current (t_m), the maximum current (i_m) and the charge content in the main oxidation peak of lead sulphate to lead dioxide on the cycled Pb–Ca–Sn electrodes

Oxidation step	t_m (*s*)	i_m (*mA cm⁻²*)	*Charge* (*mC cm⁻²*)
1. 600–1250 mV	4.2 ± 0.5	2.2 ± 0.3	7.8 ± 0.7
2. 600–1250 mV	7.4 ± 0.6	1.4 ± 0.2	9.1 ± 0.6
1. 500–1250 mV	6.7 ± 0.7	1.6 ± 0.3	9.4 ± 0.4
2. 500–1250 mV	10.6 ± 0.9	1.3 ± 0.3	9.7 ± 0.3

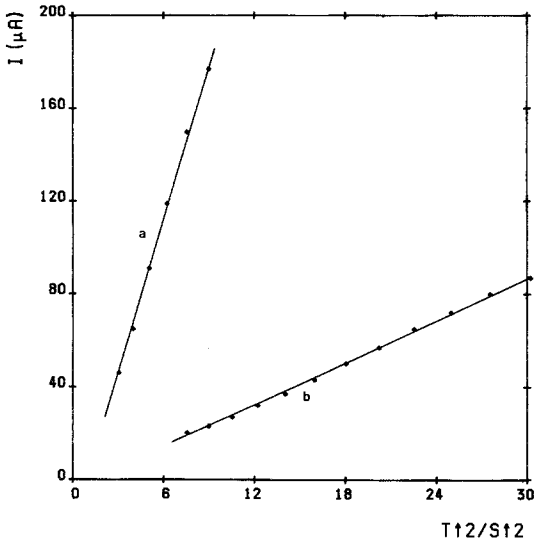

Fig. 14. Current vs t^2 for the rising part of the transient for the potentiostatic steps from 600 (a) and 500 (b) to 1250 mV.

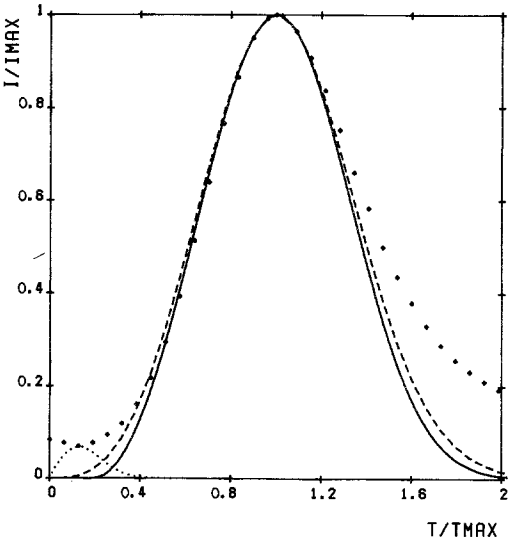

Fig. 16. (i/i_m) vs (t/t_m) for the potential step experiment from 600 to 1250 mV with the cycled lead–calcium–tin electrode: the experimental points (●●●), 2D progressive (——), 3D progressive (----), the initial 2D instantaneous (.....).

Tables 2–4). From the shapes of the transients we can conclude that the oxidation processes involved here are the same as in the case of pure lead. Because of the multilayers of $PbSO_4/PbO_2$ on the electrode formed by the prolonged cycling both the two- (Fig. 14) and three-dimensional (Fig. 15) progressive nucleation and growth mechanisms give a satisfactory correspondence. The nature of the oxidation process was further tested by plotting the i/i_m vs t/t_m data of the potentiostatic steps from 600 and 500 mV together with the dimensionless forms of Equations 1 and 2 (Figs. 16, 17). In both potentiostatic steps the three-dimensional growth of circular cones with a progressive nucleation (Equation 2) appears to correspond better to the experimental results than the two-dimensional process although the difference between the two models is not pronounced. In the case of two-dimensional growth it was

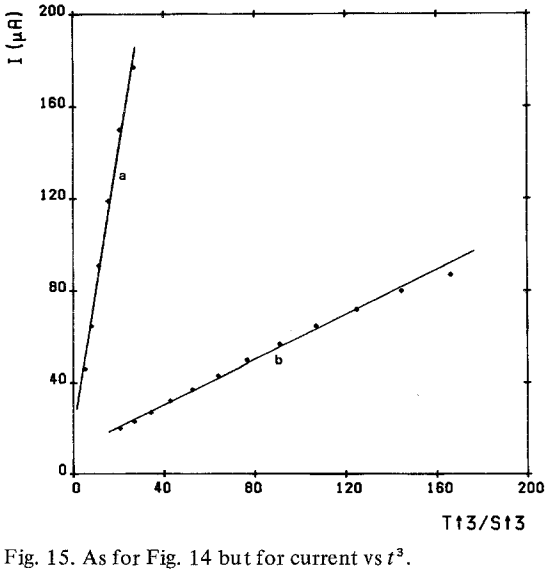

Fig. 15. As for Fig. 14 but for current vs t^3.

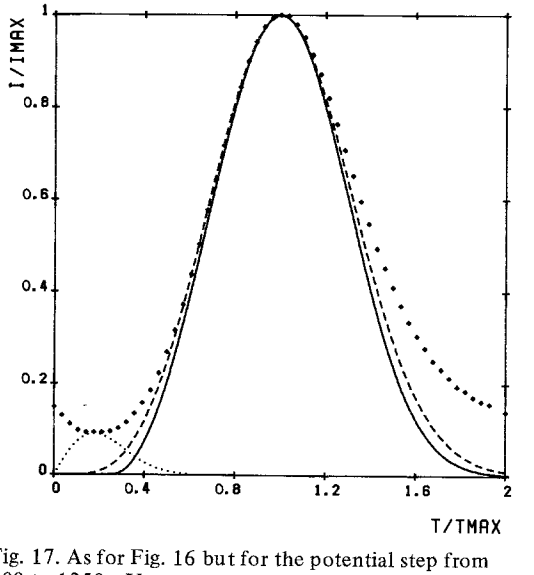

Fig. 17. As for Fig. 16 but for the potential step from 500 to 1250 mV.

necessary to add an induction time of 0.6 s in the step from 600 mV (Fig. 16) and 1.75 s in the step from 500 mV (Fig. 17) before the rise of the transient.

The separation of the initial two-dimensional instantaneous reaction shown at the beginning of the transients in Figs. 16, 17 was made with the aid of the theoretical curve corresponding to the three-dimensional process. Considering the charge content under the peaks we conclude that when a potential step is made from 600 mV the main oxidation reaction is only preceded by the conversion of some activated sites of the lead sulphate layer. In the step from 500 mV the whole monolayer is formed in the initial reaction.

In the case of the Pb–Ca–Sn alloy the deviation between the model and the experimental points at times exceeding t_m is greater than with pure lead because of the thicker PbO_2-layer formed on the electrode.

4. Conclusions

1. The thickness of the $PbSO_4/PbO_2$ layer formed during cycling between the lead sulphate (600 mV) and the lead dioxide region (1250 mV) is thicker on lead–antimony and lead–calcium–tin than on pure lead.

2. The shape of the voltammograms obtained by lead–antimony indicates a film of high porosity on the electrode.

3. In cyclic experiments the oxidation of $PbSO_4$ to PbO_2 occurs at a lower potential on the alloys than on pure lead.

4. The lack of solution speed dependence in the pulse experiments shows that the $PbSO_4$ oxidation is only limited by a solid state nucleation and growth mechanism.

5. The oxidation of lead sulphate to lead dioxide is a three-dimensional growth process with progressive nucleation on the lead and lead–calcium–tin electrodes. A possible explanation is that the orthogonal rate constant is smaller than the parallel one which gives the growth some two-dimensional character.

6. On the lead–antimony electrodes the oxidation of lead sulphate (600–1250 mV) is a reaction with instantaneous nucleation. The crystal growth is of intermediate two- and three-dimensional character.

7. Lead–antimony is sensitive to the stand time in the lead dioxide region (1250 mV) and for a shift to a more negative starting potential of the step (500 mV). In these cases the instantaneous nucleation changes with a slower progressive nucleation.

8. In the reactions with progressive nucleation a part of the electrode behaviour at the beginning of transient could be interpreted as a two-dimensional instantaneous reaction preceding the main oxidation process.

Acknowledgement

We thank Neste Battery Ltd and the Ministry of Education of Finland for financial support (to E.H.).

References

[1] M. Fleischmann and H. R. Thirsk, *Trans. Faraday Soc.* **51** (1955) 71.
[2] P. Casson, S. G. Canagaratna, N. A. Hampson and K. Peters, *J. Electroanal. Chem.* **79** (1977) 281.
[3] P. Casson, N. A. Hampson and K. Peters, *ibid.* **83** (1977) 87.
[4] N. A. Hampson, S. Kelly and K. Peters, *J. Appl. Electrochem.* **10** (1980) 261.
[5] *Idem, ibid.* **10** (1980) 91.
[6] N. A. Hampson and J. B. Lakeman, *J. Electroanal. Chem.* **107** (1980) 177.
[7] J. A. Harrison and H. R. Thirsk, *Electroanal. Chem.* **5** (1971) 67.
[8] R. D. Armstrong, M. Fleischmann and H. R. Thirsk, *J. Electroanal. Chem.* **11** (1966) 208.